Global NEST Journal, Vol 15, No 3, pp 305-314, 2013

SPATIAL AND TEMPORAL STUDY OF EXTREME PRECIPITATION OVER NORTH OF IRAN

YOUSEFI Y. [1,*]
MOHAMMADI H. [2]
AZIZI G.H. [2]
TAGHAVI F. [3]
MASOMNIA A. [4]
RORADEH H. [5]
MASOOMPOUR J. [6]

[1]*The University of Mazandaram, Mazandaran, Iran*
[2]*Faculty of Geography, University of Tehran, Tehran, Iran*
[3]*Institute of Geophysics, University of Tehran, Tehran, Iran*
[4]*Sharif University of Technology, Tehran, Iran*
[5]*The University of Mazandaran, Mazandaran, Iran*
[6]*Razi University, Kermanshah, Iran*

Received: 28/11/10
Accepted: 25/04/12
*to whom all correspondence should be addressed:
e-mail: yyousefi@ut.ac.ir

ABSTRACT
Two main focus of this study is the spatial and temporal analysis of annual 24-hour extreme precipitation amounts for different return periods, and the intra-annual variability of the frequency of month to month maximum rainfall using harmonic analysis. Data for analysis gathered from 51 stations that well-scattered at north of Iran (Caspian Sea's southern region). These data are analyzed using extreme values theory and harmonic analysis techniques. The results indicate that the Gen. Extreme Value (Jenkinson solution) is more appropriate than the linear Gumbel solution for the extreme value law. The maximum expected values of 200<x<375 mm are observed along the northern coasts of this region. The harmonic analysis showed that the highest percentage of variance for rainfall extremes explained by the first harmonic (PVR(1)) appears over western and central coastal parts. For eastern and mountainous parts PVR(3,4) is require for explain the variance.

KEYWORDS: Variability, Distribution, Frequency, Precipitation, Harmonic, PVR.

INTRODUCTION

Precipitation is one of important climatological element that varies considerably over space and time. One of the important aspects of precipitation study is the extreme precipitation. Because of economical affect, in recent years extreme climatic events have proved to be one of the most popular topics in contemporary climatology, as variation in their occurrence and intensity is seen as evidence of potential climate change (Livada and Asimakopoulos, 2005; Lupikasza, 2009). Also extreme precipitation events tend to trigger floods whose impact go beyond economic damage and involve loss of life that interest researchers to attention this topic (Pearson and Henderson, 1998). It is well understood that climatic features in precipitation records are embodied in relative variables such as monthly and annual precipitation amounts, 24-hour annual precipitation extremes and rainfall intensities and temporal scale of rainfall variation ranges from minutes in a storm cell to decades and longer. It should be mentioned that flood and drought events are mainly caused by the variability of precipitation at different scale (Garcia *et al*., 2002; Livada *et al.,* 2008; Chu *et al*., 2010). Among the precipitation features one of the most important is the periodicity of different harmonics. Worldwide, many studies have been performed to examine spatial and temporal distribution of precipitation. The seasonal distribution of precipitation, its seasonality, annual march of precipitation (Horn and Bryson, 1960), areal and temporal analysis of precipitation (Scott and Shulman, 1979), and precipitation climatology (McGee, 1969) have been analysed by means of the harmonic analysis method (Kardioğlu *et al.,* 1999). For study of meteorological variables, time series analysis is a useful tool. Generally, there are two fundamental approaches to time series analysis:

time domain analysis and frequency domain analysis. Analysis in the frequency domain involves representing data series in terms of contributions made at different time scales. Harmonic analysis is a common method in frequency domain analysis. Harmonic analysis consists of representing the fluctuations or variations in a time series as having arisen from the adding together of a series of sine and cosine functions. These trigonometric functions are harmonic in the sense that they are chosen to have frequencies exhibiting integer multiples of the fundamental frequency determined by the sample size (i.e. length) of the data series (Wilks, 2006). This method is a particularly useful tool in studying precipitation temporal patterns as it reveals the spatial variation of various precipitation characteristics. It delineates the geographic extents of various precipitation regimes and highlights the boundaries between them (Kirkyla and Hameed, 1989).

MATERIALS AND METHODS

North of Iran (Caspian Sea's southern region) is a particular region and its climate is very different. That is the remarkably short distance between Caspian Sea and Alborz Mountain chain creates very different neighboring climates in this region. For instance, Karsang and Mahmood Abad, two close stations (as shown in the Figure 1), climactically behave quite distinctively. With the aid of the well distributed network of 51 stations (Figure 1), which cover a time period of the last over 32 years an estimation of the regional distribution of mean annual precipitation can be made.

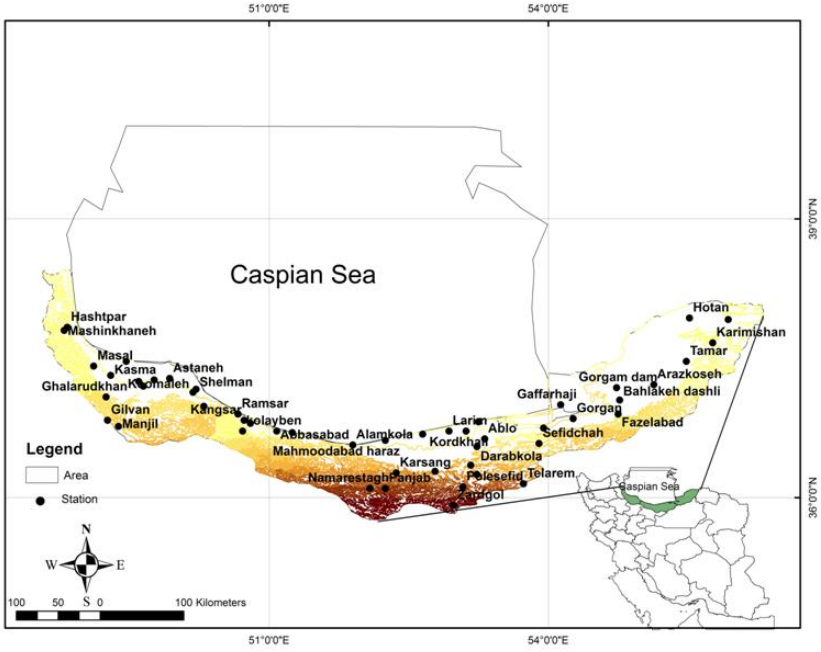

Figure 1. North of Iran with the location of stations

Stations that record precipitation in this region are governed by two organizations: Ministry of energy and Iran Meteorological Organization. For proper consideration and research 51 stations data analyzed at this work. Two methods are applied for research about extreme values in this region.

EXTREME VALUE THEORY

Extreme values are selected maximum or minimum values of sets of data. Distribution of the extreme values selected from sets of samples of any probability distribution have been shown by Fisher and Tippett (1928) to coverage to one of three forms of extreme value distributions, called Types I, II, and III, respectively, when the number of selected extreme values is large (Chow *et al*., 1998). The Three Types Theorem, originally stated without detailed mathematical proof by Fisher and Tippett (1928), and later derived rigorously by Gnedenko (1943), asserts that if a nondegenerate *H* exists (i.e., a distribution function which does not put all its mass at a single point), it must be one of three types:

$$H(x) = \exp(-e^{-x}), \qquad \text{all } x \tag{1}$$

$$H(x)=\begin{cases}0, & x<0,\\ \exp(-x^{-\alpha}) & x>0,\end{cases} \tag{2}$$

$$H(x)=\begin{cases}\exp(-|x|^{-\alpha}), & x<0,\\ 1, & x>0,\end{cases} \tag{3}$$

The three types may be combined into a single generalized extreme value (GEV) distribution (Jenkinson, 1954; Chow *et al.,* 1998; Rao and Hamed, 2000; Kotz and Nadarajah, 2000; Bali, 2003):

$$H(x)=\exp\left\{-\left(1+\xi\frac{x-\mu}{\psi}\right)_{+}^{-1/\xi}\right\} \tag{4}$$

Where μ is a location parameter, ψ > 0 is a scale parameter, and ξ is a shape parameter. The limit, ξ → 0 corresponds to the Gumbel distribution, ξ > 0 to the Frechet distribution with $\alpha=1/k$, and ξ < 0 to the Weibull distribution with $\alpha = -1/\xi$. In more informal language, the case ξ > 0 is the "long-tailed" case for which $1\text{-}H(x)\alpha x^{-1/\xi}$, ξ= 0 is the "medium-tailed" case for which 1-H(x) decreases exponentially for large x, and ξ < 0 is the "short-tailed" case, in which the distribution has a finite endpoint at $x = \mu - \psi / \xi$ (Smith, 2001).

HARMONIC ANALYSIS

For more consideration of extremes, in this paper harmonic analysis for relative frequency of 24-hour maximum precipitation occurrence for each month of the year is considered. Harmonic analysis is commonly applied to study periodic variation (Kirkyla and Hameed, 1989). The purpose of the application of harmonic analysis to the frequency of 24-hour annual maximum precipitation amounts, for each month, is the determination of the characteristic parameters of the variances of these frequencies. Harmonic analysis can also be used to indicate regions with similar annual patterns of the examined parameter (Barry and Perry, 1973). A brief explanation of the principles of harmonic analysis is presented concerning the nature and interpretation of this technique. For the monthly values of the examined frequencies $f_t (f_t=0$ at the origin), harmonic analysis can be written as follows (Jenkins and Watts, 1980; Kirkyla and Hameed, 1989; Kadioğlu *et al.,* 1999; Tarawneh and Kadioğlu, 2003; Wilks, 2006; Livada *et al.,* 2008).

$$\hat{f}_t=\bar{f}+\sum_{k=1}^{6}\left(A_k\cos\frac{360}{12}kt+B_k\sin\frac{360}{12}kt\right) \tag{5}$$

where: A_k, B_k are the coefficients of the kth harmonic (k =1, 2 . . . 6). These coefficients are given by Panofsky and Brier (1958) and Wilks (2006) as

$$A_k=\frac{1}{6}\sum_{t=1}^{6}f_t\cos\left(\frac{360}{12}kt\right) \tag{6}$$

and

$$B_k=\frac{1}{6}\sum_{t=1}^{6}f_t\sin\left(\frac{360}{12}kt\right) \tag{7}$$

where: f_t represents the monthly frequency of the annual 24-hour maximum precipitation amounts at the Tth month. The amplitude of a given harmonic is

$$C_k=\sqrt{A_k^2+B_k^2} \tag{8}$$

The variance of each harmonic can be calculated (Livada *et al.,* 2008) as:

$$V_k=\frac{C_k^2}{2} \tag{9}$$

and the percentage of variance (PVR(k)) of each harmonic can be determined by the ratio:

$$PVR(k)=V_k\Big/\sum_{1}^{n/2}V_k \tag{10}$$

The phase angle of the kth harmonic can be obtained (Wilks, 2006) by:

$$\Phi_k=\begin{cases}\tan^{-1}(B_k/A_k), & A_k>0\\ \tan^{-1}(B_k/A_k)\pm\pi, \text{ or } \pm 180°, & A_k<0\\ \frac{\pi}{2}, \text{ or } 90°, & A_k=0\end{cases} \quad (11)$$

and the date of the occurrence of the maximum of each harmonic is given by (Livada *et al.,* 2008):

$$T_k=\left(\frac{12}{360}\right)\varphi_k \quad (12)$$

The first harmonic represents a single annual cycle with the largest amplitude in comparison to the other harmonics. The second harmonic represents a probable semi-annual variation, while the third harmonic describes in more detail the seasonal 4-month variations and is also an indicator of the inter-annual patterns of the examined frequencies (Livada *et al*., 2008). Finally, the T_k values indicate the displacement of the maximum frequency along the time axis (Table 1). Harmonics indicate the dominant variation pattern of time series. If the amount of PVR (1) increases and gets closer to 1 (100 %), it explains more variation and indicates that the variation of the examined parameter would remain more regular. If the amount of the other harmonics (higher harmonics) plays a more significant role in explaining the variance, the variation of the parameter would remain less regular. Generally two first harmonics explain over 90 % of precipitation variance (Nastos and Zerefos, 2010). At this region more harmonic is require to explain of extreme precipitation variance. Six harmonics for this parameter is calculated.

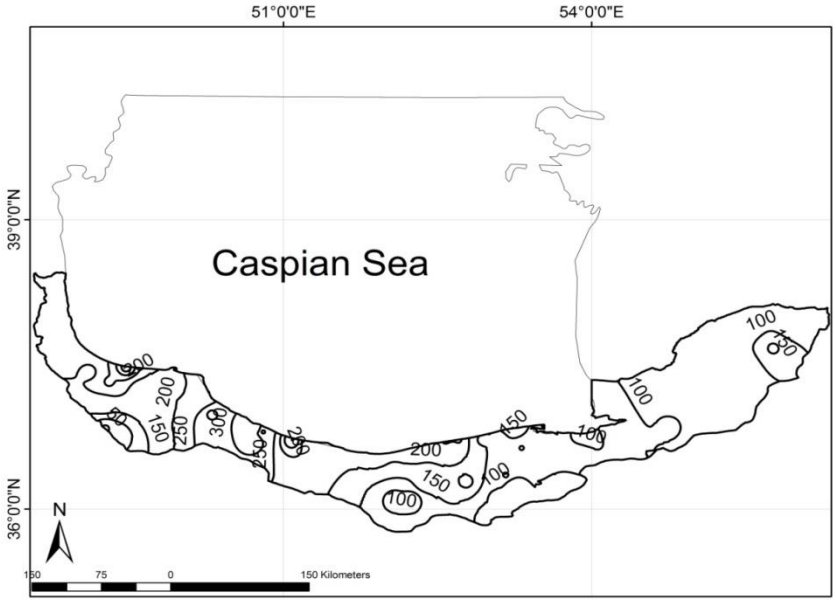

Figure 2. Contours of the expected 24-hour maximum precipitation amounts (mm) for a return period of 100 years over north of Iran using IDW (Inverse Distance Weighted)

Table 1. Relation between phase angle(expressed by the time of maximum values) and the date along the time axis (Livada et al. 2008)

T_k	-1.5	-1	-0.5	0	0.5	1	1.5
Date	1-Nov	15-Nov	1-Dec	15-Dec	1-Jan	15-Jan	1-Feb

RESULTS

Predicted 24-hour maximum precipitation amounts calculated with Gen. Extreme value distribution for a return period of 100 years are shown in figure 2. Kolmogrov-Smirnov is tested for all data that this test has good fitness with all station and not rejected. For most parts of this region, the 24-hour maximum precipitation amounts are observed usually in October or November. In mountainous and eastern parts, the 24-hour maximum precipitation amount usually occurs at May. It is clear from Fig. 2 that maximum values are observed in western and central parts, in coastal areas at this region (x>200). In mountainous and eastern parts this value is lesser than coastal parts. This pattern shows

different regime of precipitation at this region. Values of 24-hour maximum precipitation for a return period of 100 years at mountainous and eastern part are less than 120 mm. Table 2 display predicted 24-hour maximum precipitation amounts (R(T)) for T=30, 50 and 100 years, the ξ parameter of the extreme value theory, mean(u), standard deviation (σ) and the estimated absolute maximum value (|D|) of the Kolmogorov–Smirnov test, for the three representative stations.

Table 2. Predicted 24-hour maximum precipitation amounts (R(T)) for T=30, 50 and 100 years, the parameters of the extreme value theory, P-Value and the estimated absolute maximum value (|D|) of the Kolmogorov–Smirnov test, for the three representative stations

Station	R(30) (mm)	R(50) (mm)	R(100)*±Err (mm)	ξ	σ	u (mean)	max|D|	Critical value $D_{0.20}$	P-Value
Soleymantangeh $\varphi=36°15',\lambda=53°14'$**	55.6	56.8	58.0±2.001	-0.4617	12.8	35.74	0.130	<0.17909	0.75214
Maravetappeh $\varphi=37°55',\lambda=55°56'$	56	60.5	66.719±1.67	0.006	8.5	26.82	0.118	<0.16547	0.4529
Ghoran Talar $\varphi=36°17',\lambda=52°47'$	143.4	169.73	214.1±6.033	0.36599	25.9	88.9	0.111	<0.17188	0.50436

*±Error confidence intervals for 68.269% probability **φ (latitude), λ (longitude)

At the next step with aim of 51 stations data harmonic analysis of the inter-annual variability of the frequency of month-to-month maximum precipitation for north region of Iran was applied. With the separation of the data into orthogonal components, in the form of harmonics, the variation of the data can be explained. Harmonic analysis produces the maximum and minimum occurrence instances along a time axis (Livada *et al.,* 2008). Normally in the monthly data, six harmonics are adopted for application, but in practice, the first three harmonics are used over the western and central parts of region, in order to explain the variability of the examined annual frequency patterns of the 24-hour annual maximum precipitation amounts. At some research two first harmonics are applied for research (Nastos and Zerefos, 2010). The fourth and fifth harmonics represent a significant part of the total variance only in some parts of mountainous and eastern area of this region. Tables 3 to 6 give the contribution of each harmonic in four representative cases. The dominant variation is revealed by comparing the amplitudes of the six harmonics.

Table 3. Calculations of the 1st to 6th harmonic where Ak and Bk, amplitudes Ck, variances Vk, percentage of variances[PVR(k)], cumulative percentage of variances [CPVR(k)] and Tk

k	A_k	B_k	C_k	V_k	PVR_k	$CPVR_k$	φ	T_k
1	0.0486	-0.0946	0.1063	0.0057	0.7719	0.7719	-2.0936	0.048
2	-0.0130	-0.0406	0.0426	0.0009	0.1241	0.896	2.5119	-0.013
3	-0.0208	-0.0208	0.0295	0.0004	0.0593	0.9553	1.6047	-0.020
4	0.0026	0.0135	0.0138	0.0001	0.0130	0.9683	2.6369	0.002
5	0.0035	-0.0044	0.0056	0.0000	0.0021	0.9704	-1.7140	0.003
6	-0.0208	0.0000	0.0208	0.0002	0.0296	1	0.1047	-0.020
KASMA =[$\varphi=37°19',\lambda=49°18'$]								

Table 4 and Figure 3a show that for the Kasma station, the first harmonics have larger amplitude in comparison to the rest of the stations.

This is verified by the PVR(1) value which is 77 % and shows the best fit with first harmonic to the observed curve. In contrast for the Gilvan (Table 4), the first two harmonics are of the same order of magnitude.

Table 4. Calculations of the 1st to 6th harmonic where A_k and B_k, amplitudes C_k, variances V_k, percentage of variances[PVR(k)], cumulative percentage of variances [CPVR(k)] and T_k

k	A_k	B_k	C_k	V_k	PVR_k	$CPVR_k$	φ	T_k
1	0.0318	0.0408	0.0517	0.0013	0.3818	0.3818	52.089	1.74
2	0.0260	-0.0451	0.0521	0.0014	0.3876	0.7694	-60.000	-1.00
3	0.0260	-0.0260	0.0368	0.0007	0.1938	0.9632	-45.000	-0.50
4	0.0104	0.0000	0.0104	0.0001	0.0155	0.9787	0.000	0.00
5	0.0047	-0.0043	0.0064	0.0000	0.0058	0.9845	-42.626	-0.28
6	0.0104	0.0000	0.0104	0.0001	0.0155	1	0.000	0.00
GILVAN =[φ=36°50′, λ=49°01′]								

Table 5. Calculations of the 1st to 6th harmonic where A_k and B_k, amplitudes C_k, variances V_k, percentage of variances[PVR(k)], cumulative percentage of variances [CPVR(k)] and T_k

k	A_k	B_k	C_k	V_k	PVR_k	$CPVR_k$	φ	T_k
1	0.0304	-0.0161	0.0344	0.0006	0.1772	0.3818	-27.9858	-0.93
2	-0.0052	-0.0361	0.0365	0.0007	0.1992	0.3764	261.7868	4.36
3	-0.0469	-0.0365	0.0594	0.0018	0.5285	0.9048	217.8750	2.42
4	0.0104	-0.0090	0.0138	0.0001	0.0285	0.9333	-40.8934	-0.34
5	-0.0147	0.0109	0.0183	0.0002	0.0505	0.9837	143.4491	0.96
6	0.0104	0.0000	0.0104	0.0001	0.0163	1	0.0000	0.00
GORGAN =[φ=36°51′, λ=54°16′]								

Magnitude of third harmonic for Gorgan has larger amplitude (Figure 3c) and magnitude of fourth harmonic for Karimishan (Figure 3d) has larger amplitude in comparison to the rest of the stations.

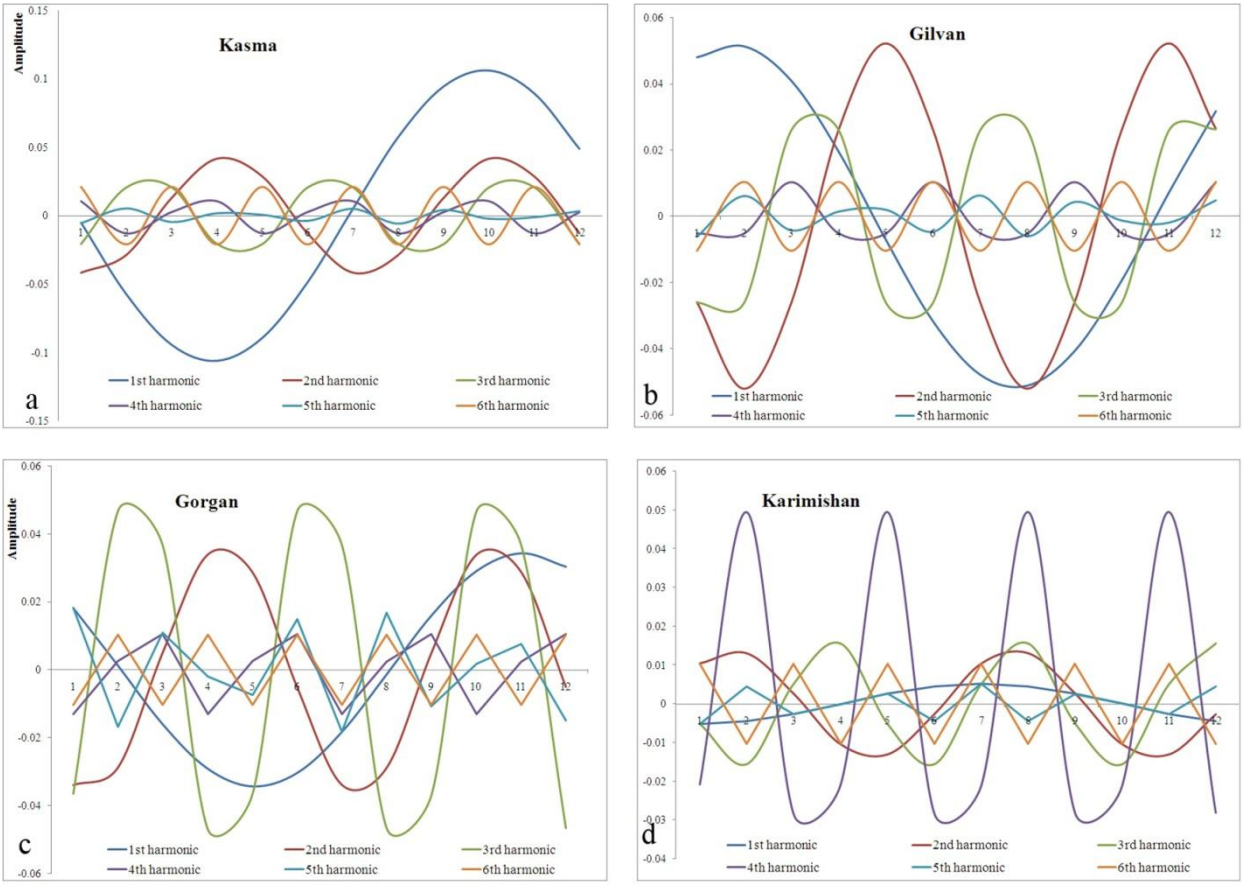

Figure 3. The calculated six harmonics for four representative stations

Table 6. Calculations of the 1st to 6th harmonic where A_k and B_k, amplitudes C_k, variances V_k, percentage of variances[PVR(k)], cumulative percentage of variances [CPVR(k)] and T_k

k	A_k	B_k	C_k	V_k	PVR_k	$CPVR_k$	ϕ	T_k
1	-0.0045	-0.0026	0.0052	0.0000	0.0088	0.3818	210	7
2	-0.0026	0.0135	0.0138	0.0001	0.0614	0.0702	100.89	1.7
3	0.0156	-0.0052	0.0165	0.0001	0.0877	0.1579	-18.43	-0.2
4	-0.0286	-0.0406	0.0497	0.0012	0.7982	0.9561	234.79	2.0
5	0.0045	-0.0026	0.0052	0.0000	0.0088	0.9649	-30	-0.2
6	-0.0104	0.0000	0.0104	0.0001	0.0351	1	180	1
KARIMISHAN=[$\varphi=37°04'$, $\lambda=55°46'$]								

First harmonic

Figure 4 shows The contours of the percentage of month to month variance PVR(1) explained by the first harmonic. The interpretation of these contours is:

1. The explanation of the first harmonic is less than 30 % in the eastern part of north of Iran, but the majority of the western particularly coastal part of this area has explanations of more than 60 %.
2. Generally the PVR(1) values decrease from north to south and west to east.
3. With increasing the distance of sea and coastal area PVR(1) values decrease.
4. PVR(1) value at the east part of this area is low. This pattern indicates that occurrence time of 24- hour maximum precipitation at eastern part is different year to year.
5. Another consequence of this pattern at this part is that the different elements are responsible for the appearance of 24-hour maximum precipitation amounts for the whole year.
6. The phase angle chart, expressed by contours of T1 values (Figure 5) for the first harmonic, show the time of maximum frequency of 24-hour extreme precipitation. The T1 values vary from September (~-3) to March (~3). Generally over mountainous region January is the time that 24-hour extreme precipitation occurs usually.

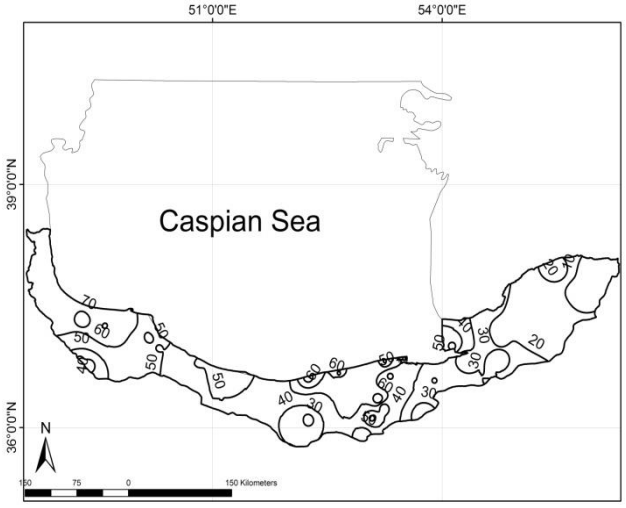

Figure 4. Contours of the percentage of variance of the first harmonic (PVR(1))

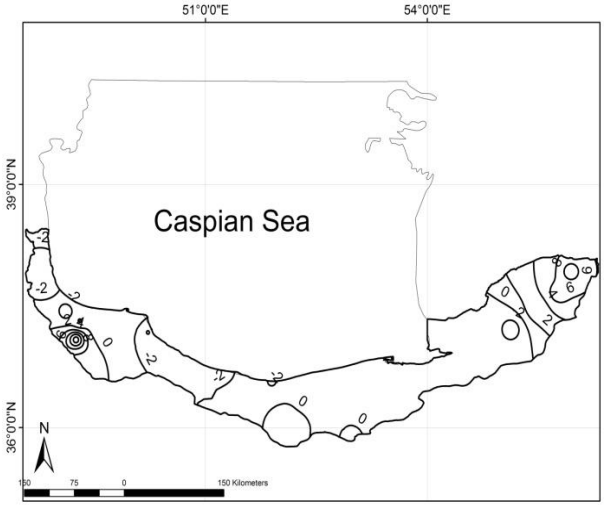

Figure 5. Contours of the phase angle of the first harmonic (T1)

Second harmonic

The spatial pattern of the second harmonic over area (Figure 6) shows that the effectiveness of the second harmonic is the same (~30 % and ~20 %) at most part of this region. At eastern and mountainous part PVR (~10 %) also is dominant.

The phase angle of the second harmonic (Figure 7) indicates that its maximum occurs usually about April. But at some area the value decrease to zero and under zero (~-1.5) that indicate the occurrence time of maximum 24-hour for second harmonic is about November.

Third harmonic

The spatial pattern of the third harmonic shows (Figure 8) that it is also effective over the eastern parts of region where three or more harmonics are needed to describe the month-to-month variation of frequencies.

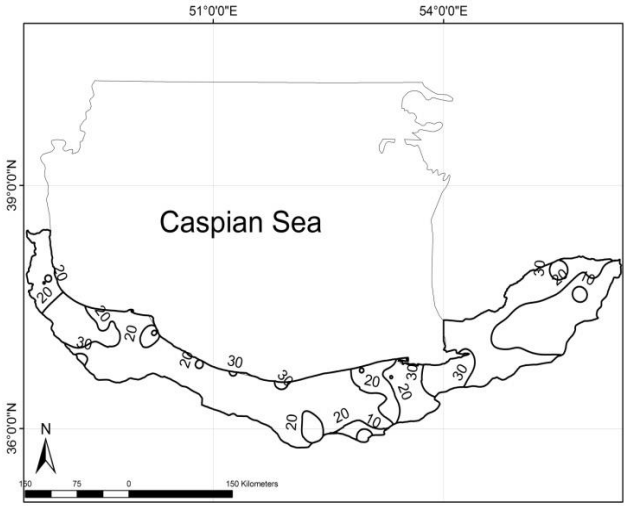

Figure 6. Contours of the percentage of variance of the second harmonic (PVR(2))

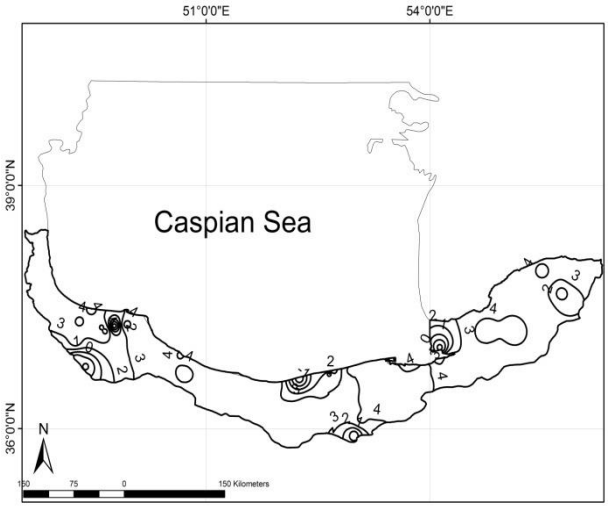

Figure 7. Contours of the phase angle of the second harmonic (T2)

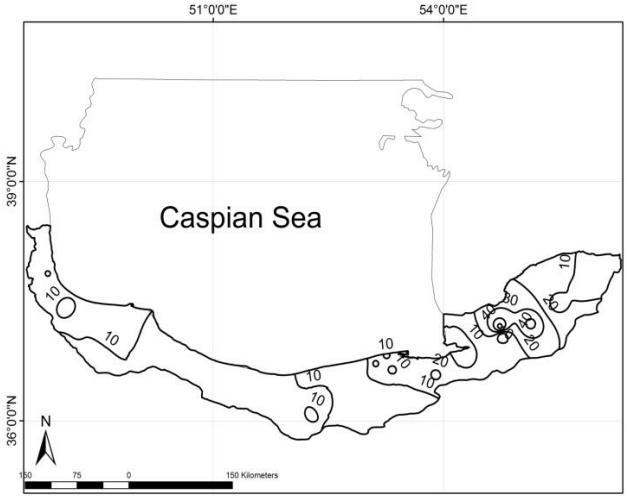

Figure 8. Contours of the percentage of variance of the third harmonic (PVR(3))

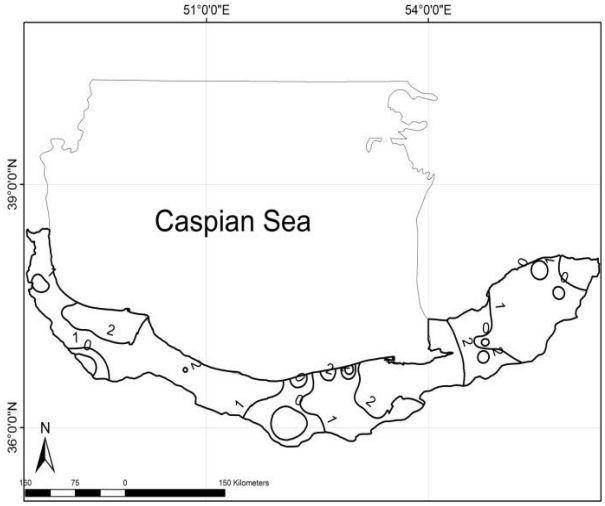

Figure 9. Contours of the phase angle of the third harmonic (T3)

Phase angle of the third harmonic (Figure 9) indicate that the maximum occurs at the coastal regions. General pattern of this phase angle is north-south. At the most area these angles decrease from coastal area to mountainous area. Time of third harmonic occurrence at most area is about March and April. Also at mountainous area and eastern part of this region this time is mid-November to mid-December.

DISCUSSION

Main objects of this paper are the spatial and temporal study of two parameters: First, on annual 24-hour extreme precipitation amounts at difference return period and second, on the inter-annual variability of the occurrence of month-to-month maximum, which was studied using harmonic analysis. From the study of the 24-hour annual maximum precipitation amounts the following conclusions were drawn:

1. For a return period of 100 years, maximum expected values (200<x<375 mm) are observed along the coast of western and central parts of this region.

2. Expected max 24-hour precipitation value for return period of 100 years, from west to east and north to south has reducing pattern. Maximum of this value is observed in coastal and western parts.

The month-to-month study of the frequency of the 24-hour annual maximum precipitation amounts showed that the highest values vary from 0.53125 to 0.125 and are observed in autumn and the mid of spring.

The annual patterns of frequency of the 24-hour annual maximum precipitation amounts are studied with the aid of harmonic analysis. The results of the estimated PVR for the first, second and third harmonics, as well as the phase angles, are plotted as contour charts from which the following conclusions can be drawn:

1. In the majority of north of Iran investigated the first harmonic explains more than the 74 % of the month-to-month variations.
2. After first harmonic second harmonic with 9.8 % has next order at explain of month-to-month variation.
3. Over the northern and central coastal parts of this region where precipitation season is autumn, extreme precipitation amounts occur during at this season. In these areas the observed values of PVR(1) and the corresponding amplitudes, which allow the definition of the annual pattern of the studied parameter, are satisfactory.
4. Over eastern parts that precipitation occurrence is chaotic, values of PVR (2,3,4) and even at some stations PVR(5,6) explain the variance. Generally the effectiveness of the second harmonic is the same for most parts of this region.
5. The first and second harmonics are significant in central and western parts, while in several cases such as Gorgan, Karimishan and Panjab (at mountainous and arid parts) the third and even the fifth harmonic are necessary for best fit to the data.
6. The time of maximum frequency occurrence for the first harmonic varies from October to March and second harmonics varies from mid-November to May, that display first harmonic is strongly related to the predominant maritime precipitation regime.

REFERENCES

Bali T.G. (2003), The generalized extreme value distribution, *Economics Letters*, **79**, 423–427.

Barry R.G. and Perry A.H., (1973), Synoptic climatological methods and applications, Methuen & Co Ltd., London.

Chow V.T., Maindment D.R. and Mays L.W., (1998), Applied hydrology, McGraw Hill, New York.

Chu J., Xia J., Xu C., Li L. and Wang Z., (2010), Spatial and temporal variability of daily precipitation in Haihe River basin, 1958–2007, *J. Geogr. Sci.*, **20**(2), 248-260.

Fisher R.A. and Tippet L.H.C., (1928), Limiting forms of the frequency distribution of the largest or smallest member of a sample, Cambridge, London.

Garcia J.A., Serrano A. and Cruz Gallego M. de la, (2002), A spectral analysis of Iberian Peninsula monthly rainfall, *Theoretical and Applied Climatology*, **71**, 77-95.

Horn L.H. and Bryson R.A., (1960), Harmonic analysis of the annual march of precipitation over the United States, *Ann*. *Assoc*. *Am*. *Geogr*., **50**, 157–171

Jenkinson A.F., (1954), The frequency distribution of the annual maximum (or minimum) values of meteorological elements, *Quarterly Royal Meteorological Society*, **81**, 158–171.

Jenkins M.G. and Watts D., (1980*),* Spectral analysis and its applications, Holden-Day, London.

Kadioğlu M., Öztürk N., Erdun H. and Şen Z., (1999), On the precipitation climatology of Turkey by harmonic analysis, *Royal Meteorological Society, International journal of climatology*, **19**, 1717–1728.

Kirkyla K. and Hameed S., (1989), Harmonic Analysis of seasonal cycle in precipitation over the United States: a comparison between observations and a general circulation model, *Journal of climate*, **2**, 1463-1475.

Kotz S. and Nadarajah S., (2000), Extreme Value Distributions Theory and Applications, London.

Livada I., Asimakopoulos D.N., (2005), Individual seasonality index of rainfall regimes in Greece, *Climate Research,* **28**, 155–161.

Livada I., Charalambous G. and Asimakopoulos D.N., (2008), Spatial and temporal study of precipitation characteristics over Greece, *Theoretical and Applied Climatology*, **93**, 45–55.

Lupikasza E., (2009), Spatial and temporal variability of extreme precipitation in Poland in the period 1951–2006, *International Journal of Climatology*, **10**, 991-1007.

McGee O.S., (1969), The use of the harmonic dial in rainfall climatology, *S*. *Afr*. *Geogr*. *J*., **51**, 65–72.

Nastos P.T. and Zerefos C.S., (2010) Cyclic modes of the intra-annual variability of precipitation in Greece, *Advance in Geosciences*, **25**, 45–50

Panofsky H.A., Brier G.W., (1958), Some applications of statistics to meteorology, Pennsylvania State University Press, Pennsylvania United States.

Pearson C.P. and Henderson R.D. (1998), Frequency distributions of annual maximum storm rainfalls in New Zealand, *Journal of Hydrology (NZ),* **37**(1), 19-33.

Rao A.R. and Hamed Khaled H., (2000), Flood frequency analysis, Taylor & Francis, United States of America.

Scott C.M. and Shulman M.D. (1979), An areal and temporal analysis of precipitation in the United States, *J*. *Appl*. *Meteor*., **18**, 627–633.

Smith R.L. (2001), Extreme values in finance, telecommunications, and the environment, Barbel Finkenstadt, Holger Rootzen, (Ed) Séminaire européen de statistique (5th: 2001: Gothenburg, Sweden), CHAPMAN & HALL/CRC, USA

Tarawneh Q and Kadioğlu M, (2003), An analysis of precipitation climatology in Jordan, *Theoretical and Applied Climatology*, **74**, 123–136.

Wilks D.S., (2006), Statistical methods in the atmospheric sciences: an introduction, Second Edition, Academic Press, San Diego.